High pressure x-ray absorption spectroscopy at lower energy in the dispersive mode: application to Ce and $FePO_4$

2005 J. Phys.: Condens. Matter 17 S883

(http://iopscience.iop.org/0953-8984/17/11/018)

INSTITUTE OF PHYSICS PUBLISHING JOURNAL OF PHYSICS: CONDENSED MATTER

J. Phys.: Condens. Matter **17** (2005) S883–S888 doi:10.1088/0953-8984/17/11/018

High pressure x-ray absorption spectroscopy at lower energy in the dispersive mode: application to Ce and $FePO_4$

J P Itié[1], F Baudelet[2], A Congeduti[1], B Couzinet[1], F Farges[3] and A Polian[1]

[1] Physique des Milieux Condensés, CNRS UMR 7602, Université Pierre et Marie Curie, 140 rue de Lourmel, 75015, Paris, France
[2] Synchrotron Soleil L'Orme des Merisiers, BP48-Saint-Aubin, F-91190, Gif sur Yvette, France
[3] Laboratoire des Géomatériaux, Université de Marne la Vallée, F-77454 Marne la Vallée cedex 2, France

Received 12 January 2005
Published 4 March 2005
Online at stacks.iop.org/JPhysCM/17/S883

Abstract

X-ray absorption spectroscopy (XAS) using a diamond anvil cell has been extended to lower energies (below 6 keV) thanks to smaller diamond anvils and to a new acquisition set-up on the energy dispersive x-ray absorption beamline of LURE. The valence change of Ce with pressure is followed at the L_{III} edge of cerium up to 8 GPa together with the bond length variation during the same experiment. The pressure induced coordination change around the Fe atom in $FePO_4$ is determined at the Fe K edge through the pre-edge feature behaviour, the XANES modification and the Fe–O bond length increase.

(Some figures in this article are in colour only in the electronic version)

1. Introduction

X-ray absorption spectroscopy (XAS) is a well adapted technique for the study of materials under high pressure [1]. This method is sensitive to structural and electronic pressure induced modifications. Moreover, XAS is a local probe around a given atom type and can also be applied to non-crystalline materials. Although XAS is compatible with large volume cells [2] and diamond anvil cells (DAC) [3], we will consider here the advantages and limitations of the DAC for performing XAS high pressure experiments.

Two different types of set-ups are available for XAS experiments: energy scanning ('classical') and energy dispersive. The first one requires a step-by-step monochromator (often a double-crystal design) where the energy scanning is obtained by the rotation of the diffracting crystals. For each energy point, the intensity of the beam is recorded before (I_0) and after the sample (I_1), the absorption corresponding to $\log(I_0/I_1)$. Therefore, the acquisition of a full

Table 1. Transmission of anvils with a total diamond thickness e for different incident photon energy.

E (keV)	$e = 2.4$ mm	$e = 1$ mm	$e = 0.5$ mm
2	6×10^{-113}	2×10^{-47}	4×10^{-24}
3	1×10^{-33}	2×10^{-14}	1×10^{-7}
4	4×10^{-14}	2.5×10^{-6}	1.5×10^{-3}
5	2×10^{-7}	2×10^{-3}	4×10^{-2}
6	2×10^{-4}	3×10^{-2}	0.17
8	3.6×10^{-2}	0.25	0.5
10	0.2	0.5	0.7

absorption spectrum requires several tens of minutes (time which can be reduced in a quick-EXAFS configuration but at the cost of a mechanics-intensive use of rotating motors). With modern x-ray optics, the beam size can be reduced to a micrometric size using mirrors and/or sagittal focusing of the second monochromator crystal. So far, because of some difficulties related to the diffraction of the diamond anvils, this type of set-up is not widely used. In fact, the dispersive mode [4, 5] has been shown to be better adapted for DAC experiments as will be shown in the next part of the paper.

2. Experimental details

High pressure experiments with the diamond anvil cell induce some limitations to x-ray absorption spectroscopy.

- The diamond diffraction induces some glitches in the spectrum.
- The size of the sample is very small (between 10 and 200 μm).
- The thickness of the sample is limited by the thickness of the gasket.
- The transmission of the diamond anvils becomes very small at low energy (see table 1).

Except for the thickness problem, these difficulties can be overcome, at least partly, using an energy-dispersive set-up and adapted anvils.

2.1. Rejection of the diamond diffraction peaks

In the dispersive set-up the acquisition of the whole spectrum is done at once in a short time (between 10 and 500 ms depending on the energy of the photons) allowing a direct observation 'live' of the spectrum. Therefore, the glitches due to the Bragg peaks of the diamond can be rejected by rotating the cell (a few degrees can be enough) with respect to the beam axis. Because it is possible to see the whole spectrum on the screen of the computer, the action of the rotation is directly controlled. Actually, using this set-up, it is possible to obtain high quality spectra with a large energy range above the threshold energy for some edges (Ni, Zn, Ga K edges). But in some cases, it is almost impossible to reject the glitches far from the threshold energy (Ge K edge for example). Therefore, if a cell position without glitches is not found, the spectra have to be recorded at two different angular positions where the glitches do not overlap and the final spectrum is obtained by combination of the two spectra. Such reconstruction is only possible when the spectrum shape is reproducible. In order to check this, we use a new acquisition mode. In the dispersive mode I_0 has to be measured independently of I_1. To reproduce the condition introduced by the DAC, I_0 is measured in an empty DAC with the same diamond size and the same gasket hole diameter. Then, this I_0 is kept in memory and

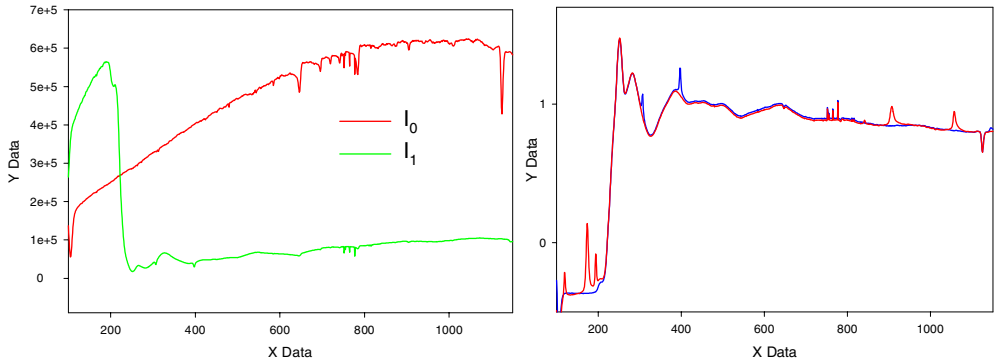

Figure 1. Left, I_0 (empty cell) and I_1 (filled cell) spectra recorded at the Mn K edge; right, x-ray absorption spectra ($\log I_1/I_0$) for two different angular positions of the DAC.

used to adjust the position of the filled cell by optimizing the shape of the absorption spectrum ($\log(I_1/I_0)$) for the first angular position (the pre-edge and the after edge mean curves have to be parallel). Then, the XAS spectrum is also kept in memory and the cell position is optimized in order to reproduce the XAS spectrum for the other angular position. This means that the two spectra are identical except for the diamond glitches (figure 1).

2.2. Small diamond anvils

In order to reduce the thickness of diamonds, it has been proposed to use perforated diamonds as support for small diamond anvils [6]. We have tested this set-up with thin diamonds ($e = 0.5$ mm) with different culet sizes. With 400 and 200 μm culets, pressure respectively up to 10 and 30 GPa have been obtained without breaking the diamonds. The total diamond thickness is reduced to 1 mm and according to table 1 experiments down to 5 keV are possible.

2.3. Small size of the sample

In high pressure experiments, the size of the sample is quite small, generally less than 200 μm in diameter. Depending on the x-ray spot size, some deformations in the spectrum shape can occur and are not always reproducible. If the spot size is larger than the sample, the spectrum is sensitive to the beam inhomogeneity. Also, if the spot size is smaller than the sample, the spectrum is sensitive to the sample inhomogeneity. The direct observation of the spectrum $\log(I_1/I_0)$ during the cell adjustment makes it possible to reproduce exactly the spectrum shape for each pressure step by comparison with the preceding one.

Therefore, combining perforated diamond anvils with the dispersive set-up, it is now possible to obtain much higher quality XAS spectra under high pressure at low energy without diamond glitches and on a large energy range above the threshold. These points will be illustrated in the next section by recent experiments performed on Ce at the L_{III} Ce edge and on $FePO_4$ at the Fe K edge.

3. Ce under high pressure

The first order phase transformation of Ce close to 0.8 GPa has been widely studied using different techniques [7, 8], including XAS [9]. Using XAS, the pressure induced modifications of the valence state can be studied through the Ce-L_{III} edge 'white line' intensity (∼5724 eV)

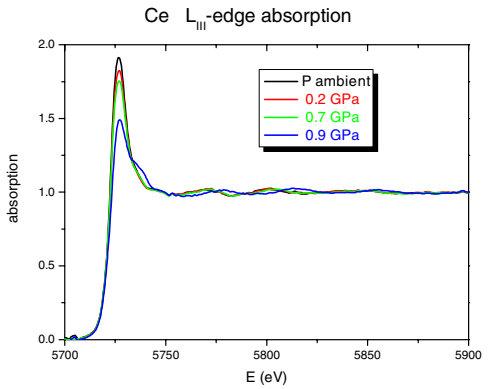

Figure 2. Evolution with pressure of the XANES spectrum of Ce at the Ce L_{III} edge.

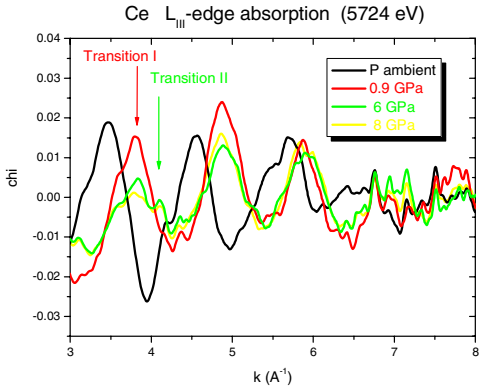

Figure 3. EXAFS oscillations of Ce at the Ce L_{III} edge for different pressures.

and those of the interatomic distances around Ce through the shift in the EXAFS oscillations. Figure 2 shows the XANES region of the absorption spectrum of Ce at the L_{III} edge for different pressures.

In this experiment, perforated diamonds supporting 500 μm thick mini-diamonds have been used for the XAS measurement in the transmission mode. The culets of the mini-diamonds were 400 μm and silicone oil was used as pressure transmitting medium. During the loading process, the cerium sample was always kept in oil in order to avoid oxidation.

Examination of figure 2 suggests that below 0.7 GPa the intensity of the 'white line' decreases, which means that the Ce valence begins to increase. In the same time, the first EXAFS oscillations are not shifted, suggesting that the Ce is still in the γ phase. At 0.9 GPa, a large drop of the white line intensity occurs with a large shift of the EXAFS oscillations, which means that, at this pressure, Ce is in the α phase. The possibility to follow both electronic (valence state) and structural (first neighbour distance) pressure induced modifications during the same experiment is a superior advantage. Above 0.9 GPa, the α phase of cerium remains stable up to 5–6 GPa, where a new transformation to the orthorhombic α' structure occurs, as seen in figure 3. Due to the orthorhombic structure, the first shell is less ordered and the intensity of the EXAFS oscillations decreases.

4. Phase transformation of $FePO_4$

$FePO_4$ belongs to the berlinite family of minerals that has been the subject of a number of investigations, mainly because of the reversible amorphization claimed for $AlPO_4$ [10]. The situation is somewhat more complicated for $FePO_4$, which undergoes a phase transformation above 2 GPa, with a coexistence of three phases in the high pressure domain [11]: a part of the sample remains in the low pressure phase, with a tetrahedral configuration around the Fe atom, a second part in a new crystalline phase ($Cmcm$, $CrVO_4$ type) and a third part in an amorphous phase. The two last phases show an octahedral configuration around the Fe atom. XAS being extremely sensitive to the local environment, this technique is well suited not only to check this result, but also to provide detailed symmetry information that cannot be probed with other methods (such as the pre-edge feature).

The pre-edge features in the absorption spectra are fingerprints of the local environment of the iron atom, particularly its local symmetry. In a tetrahedral configuration, the pre-edge

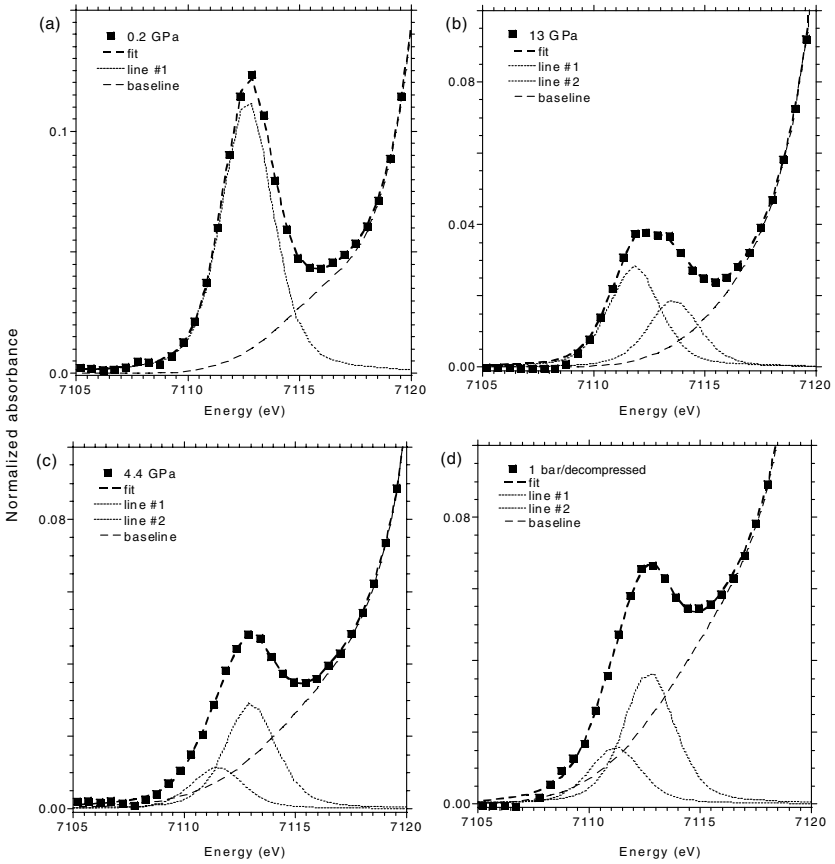

Figure 4. Pre-edge features of $FePO_4$ for different pressures.

can be approximated by a single quite intense peak. In contrast, a doublet is observed for the octahedral configuration, together with an overall lower intensity. Figure 4 shows the pre-edge features of $FePO_4$ for different pressures:

(a) $P = 0.2$ GPa $FePO_4$ is in the berlinite structure and the pre-edge corresponds to a Fe^{3+} in a T_d environment,
(b) $P = 13$ GPa $FePO_4$ is in the high pressure form and the pre-edge corresponds to a non-distorted octahedral configuration,
(c) $P = 4.4$ GPa $FePO_4$ is in the high pressure form with a small amount of the low pressure phase and the pre-edge corresponds to a distorted octahedral configuration or a mixture of tetrahedral and octahedral configurations,
(d) $P = 0$ GPa after pressurization up to 13 GPa $FePO_4$ is in the high pressure form and the pre-edge is similar to the 4.4 GPa one.

The EXAFS oscillations have been fitted for the different pressures and the Fe–O bond length has been determined. It is noticeable that a good fit is obtained only when a small amount (a few per cent) of tetrahedral configuration is added to the octahedral one. An example of such a fit is shown in figure 5 left at room pressure on decompression after a pressurization up to 13 GPa. The variation of the Fe–O main distance is shown in figure 5 (right). The results of the EXAFS fit are in agreement with the pre-edge behaviour and confirm clearly that the Fe

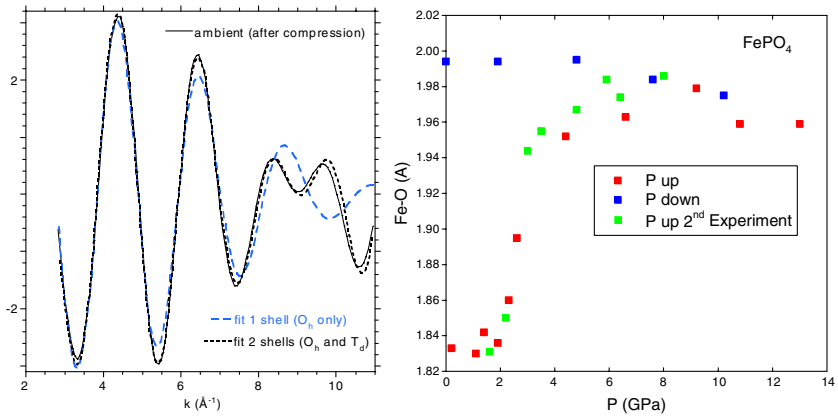

Figure 5. Left, fit of the filtered EXAFS oscillations at room pressure on decompression; right, evolution of the EXAFS-modelled average Fe–O distance with pressure.

is mainly in an octahedral configuration in the high pressure phase, with only a few per cent of tetrahedral configuration (<3% at 13 GPa) and that the transition is non-reversible.

5. Conclusion

Low energy edges are now accessible for high pressure x-ray absorption spectroscopy and therefore for high pressure x-ray magnetic circular dichroism. The k range available in the EXAFS study has been increased (up to 12 Å^{-1} for the Ni K edge). All the experiments shown here have been performed on the D11 station of DCI (LURE), a first generation synchrotron which was closed at the end of 2003. DCI will be replaced by SOLEIL in the near future (2006) where a new energy-dispersive XAS beamline Optique en Dispersion d'Energie (ODE) will be available. On this new beamline the number of photons will be increased by three orders of magnitude compared to the D11 beamline and will be focused in a 20 μm $\times$ 20 μm spot as is the case actually in the ID24 energy-dispersive absorption beamline of ESRF.

References

[1] Itié J P 2004 *High Pressure Crystallography* ed A Kastrusiak and P McMillan (Dordrecht: Kluwer–Academic) p 257
[2] Buontempo U, Filipponi A, Martinez-Garcia D, Postorino P, Mezouar M and Itié J P 1998 *Phys. Rev. Lett.* **80** 1912
[3] Itié J P 1992 *Phase Transit.* **39** 81
[4] Tolentino H, Baudelet F, Dartyge E, Fontaine A, Lena A and Tourillon G 1990 *Nucl. Instrum. Methods* A **289** 307
[5] Pascarelli S, Nelsius T, DePanfilis S, Bonfim M, Pizzini S, McKay K, David S, Fontaine A, San-Miguel A, Itié J P, Gauthier M and Polian A 1999 *J. Synchrotron. Radiat.* **6** 146
[6] Dadashev A, Pasternak M P, Rozenberg G Kh and Taylor R D 2001 *Rev. Sci. Instrum.* **72** 2633
[7] Staun-Olsen J, Gerward L, Benedict U and Itié J P 1985 *Physica* B **133** 129
[8] Jeong I-K, Darlng T W, Graf M J, Proffen Th, Heffner R H, Lee Y, Vogt T and Jorgensen J D 2004 *Phys. Rev. Lett.* **92** 105702
[9] Röhler J 1984 *EXAFS and Near Edge Structures III* ed K O Hodgson, B Hedman and J E Penner-Hahn (Berlin: Springer) p 379
[10] Kruger M B and Jeanloz R 1990 *Science* **249** 647
[11] Pasternak M P, Rozenberg G Kh, Milner A P, Amanowicz M, Zhou T, Schwartz U, Taylor R D, Hanfland M and Brister K 1997 *Phys. Rev. Lett.* **79** 4409